Provided for non-commercial research and education use.
Not for reproduction, distribution or commercial use.

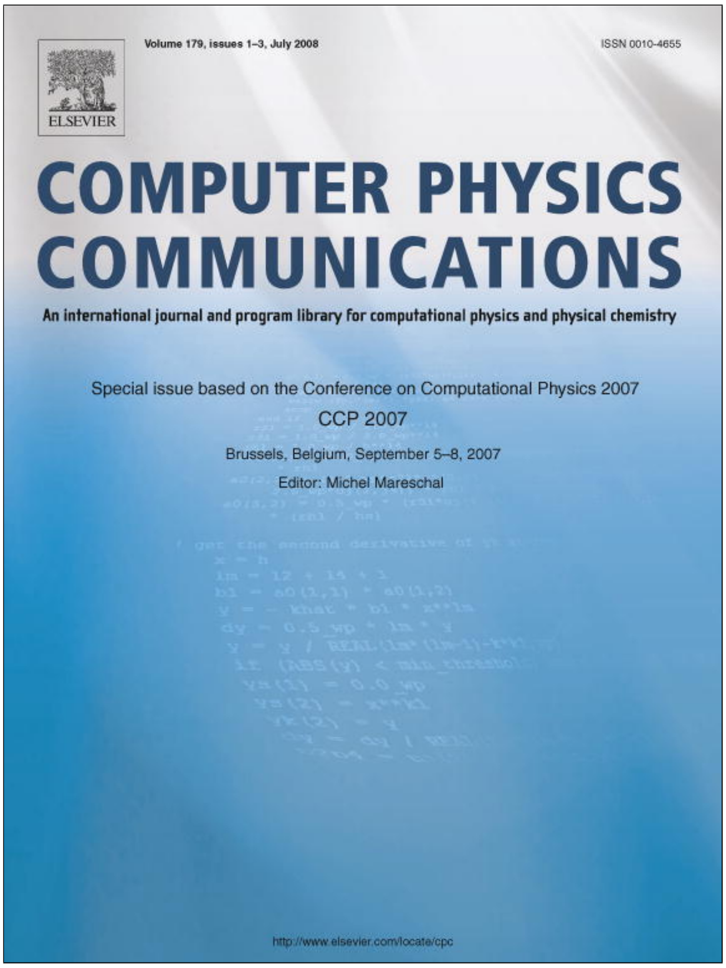

Volume 179, issues 1–3, July 2008

ISSN 0010-4655

ELSEVIER

COMPUTER PHYSICS COMMUNICATIONS

An international journal and program library for computational physics and physical chemistry

Special issue based on the Conference on Computational Physics 2007

CCP 2007

Brussels, Belgium, September 5–8, 2007

Editor: Michel Mareschal

http://www.elsevier.com/locate/cpc

This article appeared in a journal published by Elsevier. The attached copy is furnished to the author for internal non-commercial research and education use, including for instruction at the authors institution and sharing with colleagues.

Other uses, including reproduction and distribution, or selling or licensing copies, or posting to personal, institutional or third party websites are prohibited.

In most cases authors are permitted to post their version of the article (e.g. in Word or Tex form) to their personal website or institutional repository. Authors requiring further information regarding Elsevier's archiving and manuscript policies are encouraged to visit:

http://www.elsevier.com/copyright

Author's personal copy

Available online at www.sciencedirect.com

ScienceDirect

Computer Physics Communications 179 (2008) 132–139

Computer Physics Communications

www.elsevier.com/locate/cpc

Reactive multiparticle collision dynamics

Katrin Rohlf [a], Simon Fraser [b], Raymond Kapral [b,*]

[a] Department of Mathematics, Ryerson University, 350 Victoria Street, Toronto, ON M5B 2K3, Canada
[b] Chemical Physics Theory Group, Department of Chemistry, University of Toronto, Toronto, ON M5S 3H6, Canada

Available online 30 January 2008

Abstract

A mesoscopic dynamics method for the simulation of spatially distributed chemically reacting systems under equilibrium and nonequilibrium conditions is described. Non-reactive collisions are modeled by multiparticle collision dynamics that conserves mass, momentum and energy. Reactive collisions are described by birth–death stochastic processes. The dynamics is governed by a Markov chain in the full phase space of the system, which reduces to mass action rate laws in the mean field limit. Simulations on the Selkov model are carried out to illustrate the simulation method.

© 2008 Elsevier B.V. All rights reserved.

PACS: 82.20.Fd; 05.40.-a

Keywords: Chemical reactions; Mesoscopic model; Multiparticle collision dynamics

1. Introduction

When viewed on mesoscopic scales, chemically reacting systems may exhibit behavior that is different from that seen on macroscopic scales. Normally, such systems are described macroscopically by chemical rate laws or reaction–diffusion equations. These descriptions assume that the system contains large numbers of reactive molecules and, in the case of the reaction–diffusion equation, that spatial gradients are weak. There are many instances where such descriptions are likely to be inappropriate. Consider biochemical reactions occurring in a cell [1]. Cells are small chemical reactors with volumes often in the range of μm^3. Some chemical species may have very low concentrations, so that there may be only a few molecules of these species present in the cell. Similar considerations apply to reactions taking place in micelles in microemulsion solutions or to reactions in other nano-confined systems. In such circumstances, macroscopic continuum approaches will fail and models that account for the discrete nature of the chemical species and molecular fluctuations must be used.

The most direct way to account for all of these features is to follow the reactive dynamics at a microscopic level using molecular dynamics (MD). However, the simulation of chemical reactions in a solvent or dense background medium presents computational problems. The large population of solvent particles, while chemically inert, influences the overall dynamics and evolution of the system through collisions, even when reactive events are rare. This makes the Hamiltonian dynamics of large systems computationally challenging. Consequently, a variety of approximate or coarse grain methods are usually employed to investigate such systems.

For spatially uniform systems, the birth–death master equation, where reactions occur with given probabilities, can be used to model the reactive dynamics in a way that incorporates the effects of fluctuations in the numbers of chemical species [2]. Gillespie's algorithm provides an efficient way to simulate the dynamics [3,4]. Often, it is essential to account for spatial degrees of freedom in the system. In this case, one may use reaction–diffusion equations or spatial master equations where birth–death reaction dynamics is combined with diffusive hops among spatial cells to account for both species number fluctuations and diffusion [5–10].

At a very basic level, the molecules in a reactive system move from point to point and interact or collide in non-reactive or reactive collisions that change their velocities and possibly their identities or species numbers. At a mesoscopic level, often the full details of the interactions are not important. In such

---

[*] Corresponding author.
E-mail address: rkapral@chem.utoronto.ca (R. Kapral).

0010-4655/$ – see front matter © 2008 Elsevier B.V. All rights reserved.
doi:10.1016/j.cpc.2008.01.027

Author's personal copy

cases one may consider coarse grain versions of the collision process that mimic the effects of many real collisions; however, the coarse grained collisions cannot be constructed in an arbitrary fashion. It is important that they preserve the essential properties of the real collision dynamics. In this article we consider the extension of one such mesoscopic dynamical scheme, multiparticle collision (MPC) dynamics [11–13], to chemically reactive systems. MPC dynamics conserves mass, momentum and energy. The dynamics also preserves phase space volumes. On long distance and time scales one may show that the system obeys the Navier–Stokes equations of hydrodynamics. The transport coefficients are easily computed for this model [12,15,16]. Furthermore, MPC dynamics can be combined with molecular dynamics of embedded solute molecules or particles. In such hybrid MPC-MD schemes, hydrodynamic interactions among the solute molecules are automatically taken into account since momentum is conserved. As a result of these features, MPC dynamics has been used to simulate a variety of systems [13] including hydrodynamic flows [17], colloid [18] and polymer [19,20] systems and self-propelled particles [21,22].

The extension of MPC dynamics presented here provides a mesoscopic basis for the study of general spatially distributed reactive systems in equilibrium as well as far-from-equilibrium conditions. It naturally includes local and global species number fluctuations. The dynamics reduces to the reaction–diffusion equation on long distance and time scales.

The outline of the paper is as follows: In Section 2 we present the extension of MPC dynamics to reactive systems and give an algorithm for the simulation of the dynamics. The formulation allows for the possibility of reactions driven far from equilibrium by flows of chemicals so that particle numbers are no longer conserved. In Section 3, we show how the mean field chemical rate laws are obtained on macroscopic scales for a specific biochemical reaction, the Selkov model, carried out under far-from-equilibrium conditions. Section 4 presents the results of simulations of the Selkov model in order to illustrate the features of the method. The conclusions are given in Section 5, while extensions of reactive collision rules that conserve mass, momentum and energy, which may be useful for studies of reactive fluid flows or in other contexts, are given in Appendix A.

2. Reactive multiparticle collision dynamics

Multiparticle collision dynamics accounts for the two basic elements discussed above: particle motion and collisions. Suppose that in a system of N molecules in a volume V the ith molecule has position $\mathbf{x}_i$ and velocity $\mathbf{v}_i$. Effective multiparticle collisions are assumed to take place at discrete time intervals τ. Between such collisions molecules free stream. Multiparticle collisions are carried out in the following way: at each time interval τ the system with volume V is divided into N_c cells of volume V_c so that $V = N_c V_c$. Rotation operators $\hat{\omega}_\xi$, chosen from some set of rotation operators, $\varOmega = \{\hat{\omega}_1, \ldots, \hat{\omega}_n\}$, are assigned to each cell $\mathcal{V}_\xi$ of the system. If $\mathbf{V}_\xi$ is the center of mass velocity of all molecules in cell $\mathcal{V}_\xi$, collisions change particle velocities, $\mathbf{v}_i$, for $\mathbf{x}_i \in \mathcal{V}_\xi$, according to the multiparticle collision rule, $\mathbf{v}_i' = \mathbf{V}_\xi + \hat{\omega}_\xi(\mathbf{v}_i - \mathbf{V}_\xi)$, where $\mathbf{v}_i'$ is the post-collision velocity. This collision rule can be generalized to multi-component systems [14]. If $\ell_i \in \{1, 2, \ldots, s\}$ denotes the species label of particle i, then we may write the collision rule as

$$\mathbf{v}_i' = \mathbf{V}_\xi' + \hat{\omega}_\xi\big(\mathbf{V}_\xi^{\ell_i} - \mathbf{V}_\xi\big) + \hat{\omega}_\xi^{\ell_i}\hat{\omega}_\xi\big(\mathbf{v}_i - \mathbf{V}_\xi^{\ell_i}\big), \tag{1}$$

where $\mathbf{V}_\xi^{\ell_i}$ is the center of mass velocity of particles of species ℓ_i in cell $\mathcal{V}_\xi$ and $\hat{\omega}_\xi$ and $\hat{\omega}_\xi^{\ell_i}$ are again randomly chosen rotation operators. At each collision update $\hat{\omega}_\xi$ acts on all particles in $\mathcal{V}_\xi$ and then $\hat{\omega}_\xi^{\ell_i}$ acts on the subsets of particles of species ℓ_i in $\mathcal{V}_\xi$. As noted above, it can be shown that this collision rule conserves mass, momentum and energy and preserves phase space volumes.

Using the MPC rule, the transport properties of the system can be computed. An especially relevant transport property for the reactive systems we consider is the diffusion coefficient. Taking the collision rule that treats all non-reactive collisions among different species as being the same, the diffusion coefficient can be expressed as a discrete-time Green–Kubo formula. For rotations about a randomly chosen axis by angles of $\pm\alpha$ the diffusion coefficient can be evaluated approximately to give [14],

$$D = \frac{k_B T \tau}{2m}\left(\frac{3\gamma}{(\gamma - 1 + e^{-\gamma})(1 - \cos\alpha)} - 1\right), \tag{2}$$

where γ is the average number of particles per collision cell and m is the mass of each particle.

Next, we need to account for the possibility that chemical reactions may take place among the species. Reactions are assumed to occur locally within each cell by birth–death stochastic processes. We first consider a simple birth–death description for an open system that may be far from equilibrium. In this case the reactive events will not, in general, satisfy mass, momentum and energy conservation. In Appendix A we show how reactive rules can be constructed that do satisfy all conservation laws. Such a generalization may be especially useful when coupling between reaction and fluid flow is of interest or when hydrodynamic interactions among solute molecules must be taken into account.

Consider a set of reactions with reaction R_μ characterized by rate constant k_μ:

$$R_\mu: \sum_{\ell=1}^{s} \nu_\ell^\mu X_\ell \xrightarrow{k_\mu} \sum_{\ell=1}^{s} \bar{\nu}_\ell^\mu X_\ell \quad (\mu = 1, \ldots, r), \tag{3}$$

where X_ℓ ($\ell = 1, \ldots, s$) are the s chemical species and ν_ℓ^μ and $\bar{\nu}_\ell^\mu$ are the stoichiometric coefficients for reaction μ. Suppose that there are N_ℓ^ξ particles of species ℓ in cell $\mathcal{V}_\xi$, giving a total number of $N^\xi = \sum_\ell N_\ell^\xi$ particles in the cell. We assume that reactions occur independently in the cells. The probability that a reaction R_μ will occur in $\mathcal{V}_\xi$ in $(t, t + dt)$ is $k_\mu(V_c) h_\mu^\xi \, dt \equiv a_\mu^\xi \, dt$. The factor a_μ^ξ for a randomly chosen reaction R_μ in $\mathcal{V}_\xi$ is given by

$$a_\mu^\xi = k_\mu(V_c) \prod_{\ell=1}^{s} \frac{N_\ell^\xi!}{(N_\ell^\xi - \nu_\ell^\mu)!} \equiv k_\mu(V_c) h_\mu^\xi, \tag{4}$$

Author's personal copy

where the notation $k_\mu(V_c)$ indicates that the rate constants have been scaled for the cell volume V_c and h_μ^ξ is the combinatorial factor that accounts for the number of different ways the reaction can occur in the cell. In this simple model, reactions occur with probabilities that are independent of the particle velocities. This need not be the case and it is not difficult to generalize this rule. In particular, it is possible to account for activated reactive events that depend on the energies of the particles. The combinatorial factor $h_\mu^\xi = 0$ if $\nu_\ell^\mu > N_\ell^\xi$ for any ℓ, so reaction R_μ cannot occur in cell $\mathcal{V}_\xi$ in this case; clearly $a_\mu^\xi = 0$ also. The probability that no reaction will occur in the time t' is $\mathcal{P}_0^\xi(t') = e^{-a_0^\xi t'}$, where $a_0^\xi = \sum_\nu a_\nu^\xi$. The probability density that no reaction will occur up to the time t' and the reaction R_μ will occur between t' and $t' + dt'$ is $\mathcal{P}_\mu^\xi(t') = a_\mu^\xi e^{-a_0^\xi t'}$. In reactive multiparticle collision (RMPC) dynamics, reactive and non-reactive collision occur at discrete time intervals τ. Consequently, the probability that in the time interval τ the reaction R_μ will occur first, followed by any other events, is of interest and is given by

$$p_\mu^\xi(\mathbf{N}^\xi, \tau) = \int_0^\tau dt'\, \mathcal{P}_\mu^\xi(t') = \frac{a_\mu^\xi}{a_0^\xi}\left(1 - e^{-a_0^\xi \tau}\right), \tag{5}$$

where $\mathbf{N}^\xi$ is the vector of species populations in the cell. The dependence on τ will be omitted when confusion is unlikely to arise. This quantity may be used to sample reactive events at the discrete times τ. If the reaction probability is small so that $a_0^\xi \tau \ll 1$, then $p_\mu^\xi(\mathbf{N}^\xi) = a_\mu^\xi \tau$, which is the correct form for only one reactive event in the time interval τ. Should $a_0^\xi \tau$ not satisfy this inequality, the full expression for $p_\mu^\xi(\mathbf{N}^\xi)$ will provide a sampling function that is bounded by unity.

In summary, in RMPC dynamics, at time intervals τ the system is divided into collision cells and reactive multiparticle collisions are carried out independently in each cell. These collisions consist of the concatenation of MPC velocity-changing collisions and birth–death stochastic reactive events that take place with probabilities $p_\mu^\xi(\mathbf{N}^\xi)$. The combination of reactions and multiparticle collisions models coarse grain reactive and non-reactive collisions in the system. Particles then free stream for a time τ until the next collision event.

The above dynamics defines a Markov chain for a probability density $P(\mathbf{x}^N, \mathbf{v}^N, t)$, where N is the total number of particles in the system at time t and $(\mathbf{x}^N, \mathbf{v}^N) = (\mathbf{x}_1, \ldots, \mathbf{x}_N, \mathbf{v}_1, \ldots, \mathbf{v}_N)$ are the phase-space coordinates. We use the notation: $\mathbf{v}^N = \prod_{\xi=1}^{N_c} \prod_{\ell=1}^{s} \mathbf{v}_1 \mathbf{v}_2 \ldots \mathbf{v}_{N_\ell^\xi} = \prod_{\xi=1}^{N_c} \prod_{\ell=1}^{s} \mathbf{v}^{N_\ell^\xi}$, etc. The Markov Chain can be written formally as

$$\begin{aligned} P(\mathbf{x}^N + \mathbf{v}^N \tau, \mathbf{v}^N, t + \tau) &= e^{i\mathcal{L}_0 \tau} P(\mathbf{x}^N, \mathbf{v}^N, t + \tau) \\ &= (\hat{\mathcal{R}} \hat{\mathcal{C}} P)(\mathbf{x}^N, \mathbf{v}^N, t), \end{aligned} \tag{6}$$

where $\hat{\mathcal{R}}$ and $\hat{\mathcal{C}}$ are operators that correspond to the reactive and MPC events, respectively, and the free streaming operator is $i\mathcal{L}_0 = \mathbf{v}^N \cdot \nabla_{\mathbf{x}^N}$. The RMPC operator has the formal structure

$$\begin{aligned} &(\hat{\mathcal{R}} \hat{\mathcal{C}} P)(\mathbf{x}^N, \mathbf{v}^N, t) \\ &\quad = \frac{1}{|\mathcal{R}|^{N_c}} \sum_{\mathcal{R}^{N_c}} \frac{1}{|\Omega|^{N_c}} \sum_{\Omega^{N_c}} \left(\left(\prod_{\xi=1}^{N_c} \hat{\mathcal{R}}^\xi \hat{\mathcal{C}}^\xi \right) P \right)(\mathbf{x}^N, \mathbf{v}^N, t), \end{aligned} \tag{7}$$

where $\mathcal{R}$ is a set of reactions, $\mathcal{R} = \{R_0, R_1, \ldots, R_r\}$, including the possibility of no reaction denoted by R_0. The probability that no reaction occurs in the time interval τ is $p_0^\xi(\mathbf{N}) = 1 - \sum_{\mu=1}^{r} p_\mu^\xi(\tau) = e^{-a_0^\xi \tau}$. Eq. (7) expresses the fact that the RMPC operators act independently on each collision cell and the values of the velocity rotation operators are chosen from the set Ω and the reaction operators are chosen from $\mathcal{R}$. The collision operators have the following more explicit expressions: For notational simplicity, we assume that the multiparticle collisions are not species dependent. In this case we can write [11,12]

$$\begin{aligned} P^C(\mathbf{x}^{N'}, \mathbf{v}^{N'}, t) = (\hat{\mathcal{C}} P)(\mathbf{x}^{N'}, \mathbf{v}^{N'}, t) &= \frac{1}{|\Omega|^{N_c}} \sum_{\Omega^{N_c}} \int d\mathbf{v}'^{N'} P(\mathbf{x}^{N'}, \mathbf{v}'^{N'}, t) \\ &\quad \times \prod_{i=1}^{N'} \delta\big(\mathbf{v}_i - \mathbf{V}_\xi - \hat{\omega}_\xi(\mathbf{v}'_i - \mathbf{V}_\xi)\big). \end{aligned} \tag{8}$$

Here we use N' to denote the number of particles in the system at time t prior to the action of the reaction operators. The reaction operator is easily written for the case where the reactive events involve individual particles in the cells [23], rather than simply acting on the species numbers in the cells. In its simplest form considered here, we assume that particles within the cells are not distinguished in reactive events. In this case, the full RMPC operator may now be written more explicitly as

$$\begin{aligned} &(\hat{\mathcal{R}} P^C)(\mathbf{x}^N, \mathbf{v}^N, t) \\ &\quad = \sum_{\mathbf{N}'} \prod_{\xi=1}^{N_c} \sum_{\mu=0}^{r} p_\mu^\xi(\mathbf{N}'^\xi) \\ &\qquad \times \prod_{\ell=1}^{s} \delta_{N_\ell^\xi, N_\ell'^\xi + \Delta_\ell^\mu} \prod_{k=1}^{-\Delta_\ell^\mu} \int d\mathbf{x}_{N_\ell^\xi + k}\, d\mathbf{v}_{N_\ell^\xi + k} \\ &\qquad \times \prod_{j=1}^{\Delta_\ell^\mu} \frac{1}{V_c} \phi_0(\mathbf{v}_{N_\ell'^\xi + j}) P^C(\mathbf{x}^{N'}, \mathbf{v}^{N'}, t), \end{aligned} \tag{9}$$

where the Maxwell distribution, for particle mass unity, is $\phi_0(\mathbf{v}) = (2\pi k_B T)^{-3/2} \exp(-|\mathbf{v}|^2 / 2k_B T)$ and $\Delta_\ell^\mu = \bar{\nu}_\ell^\mu - \nu_\ell^\mu$. We use the convention that if the upper limit in the product is less than the lower limit the product is to be interpreted as unity. The delta functions specify the species number changes in reactive events. If particles are created in a reaction, their velocity is chosen from a Maxwell distribution at the temperature of the system. These equations generalize the treatment of cubic autocatalysis fronts considered earlier [24] to arbitrary reacting systems and form the basis for the analysis of the RMPC dynamics.

3. Derivation of mean field equation for Selkov model

In order to illustrate the use and simulation of RMPC dynamics, we consider the reversible version of the Selkov reac-

Author's personal copy

tion [25],

$$R_1: A \xrightarrow{k_1} X, \qquad R_2: X \xrightarrow{k_2} A, \qquad R_3: X+2Y \xrightarrow{k_3} 3Y,$$
$$R_4: 3Y \xrightarrow{k_4} X+2Y, \qquad R_5: Y \xrightarrow{k_5} B, \qquad R_6: B \xrightarrow{k_6} Y. \quad (10)$$

This reaction scheme is a very simplified model of the phosphofructokinase portion of the glycolytic cycle that contributes to the oscillations seen in this system. Using a reactive lattice-gas model [26,27], it was studied in the context of biochemical reactions at the cellular level [28]. Since the mean field reaction dynamics of the reversible version of the model shows both oscillatory and steady state behavior and the mean field phase diagram is known [29], it is a convenient test case for our study. The chemical rate law corresponding to Eq. (10) is

$$\frac{dc_X(t)}{dt} = k_1 - k_2 c_X - k_3 c_X c_Y^2 + k_4 c_Y^3,$$
$$\frac{dc_Y(t)}{dt} = k_3 c_X c_Y^2 - k_4 c_Y^3 - k_5 c_Y + k_6. \quad (11)$$

To demonstrate the ability of our methods to allow for changes in the total number of particles in time, we consider an open chemical system for which the concentrations of A and B particles are kept fixed through external controls. In writing Eq. (11) we have incorporated the constant concentration c_A into the rate constant k_1 and the constant concentration c_B into the rate constant k_6. This means X particles are added through R_1 with constant rate k_1, and Y particles are added with constant rate k_6 through R_6, while reactions R_2 and R_5 remove X and Y particles from the system respectively. In terms of our previous notation, $r = 6$, and $s = 2$. We will denote $X_1 = X$ and $X_2 = Y$ going forward.

We now show how RMPC dynamics can be reduced to the mass action rate law when non-reactive collisions occur much more frequently than reactive collisions. In this case the velocity distribution is Maxwellian and diffusion is rapid so that the system is spatially homogeneous so that the particle distribution is Poissonian. Under these conditions RMPC dynamics reduces to birth–death Markov chain dynamics for the species numbers.

Assuming that non-reactive events are effective enough to decorrelate the particles in the system, we write P as a product of local probability distributions,

$$P(\mathbf{x}^{N'}, \mathbf{v}^{N'}, t) = \prod_{\xi=1}^{N_c} P_0^\xi(\mathbf{x}^{N'^\xi}, \mathbf{v}^{N'^\xi}), \quad (12)$$

that are locally Poissonian number-distributed and have a Maxwell velocity distribution. Thus,

$$P_0^\xi(\mathbf{x}^{\mathbf{N}'^\xi}, \mathbf{v}^{\mathbf{N}'^\xi}) = \tilde{P}(\mathbf{N}'^\xi) \prod_{l=1}^{N'^\xi} \frac{1}{V_c} \phi_0(\mathbf{v}_l), \quad (13)$$

where

$$\tilde{P}(\mathbf{N}^\xi) = e^{-\overline{N}_X} \frac{\overline{N}_X^{N_X^\xi}}{N_X^\xi!} e^{-\overline{N}_Y} \frac{\overline{N}_Y^{N_Y^\xi}}{N_Y^\xi!} \quad (14)$$

is a product of Poissonian distributions for each species. Then, integration of Eq. (6) for the scheme (9) over all variables except the local number of particles in cell ξ leads to

$$\begin{aligned}
\tilde{P}(N^\xi, t+\tau) &= \bar{k}_1(\tau)\tilde{P}\big(N_X^\xi - 1, N_Y^\xi\big) + \bar{k}_2(\tau)\big(N_X^\xi + 1\big)\tilde{P}\big(N_X^\xi + 1, N_Y^\xi\big) \\
&\quad + \bar{k}_3(\tau)\big(N_X^\xi + 1\big)\big(N_Y^\xi - 1\big)\big(N_Y^\xi - 2\big)\tilde{P}\big(N_X^\xi + 1, N_Y^\xi - 1\big) \\
&\quad + \bar{k}_4(\tau)\big(N_Y^\xi + 1\big)N_Y^\xi\big(N_Y^\xi - 1\big)\tilde{P}\big(N_X^\xi - 1, N_Y^\xi + 1\big) \\
&\quad + \bar{k}_5(\tau)\big(N_Y^\xi + 1\big)\tilde{P}\big(N_X^\xi, N_Y^\xi + 1\big) \\
&\quad + \bar{k}_6(\tau)\tilde{P}\big(N_X^\xi, N_Y^\xi - 1\big) \\
&\quad + \big(1 - \bar{k}_1(\tau) - \bar{k}_2(\tau)N_X^\xi - \bar{k}_3(\tau)N_X^\xi N_Y^\xi\big(N_Y^\xi - 1\big) \\
&\quad - \bar{k}_4(\tau)N_Y^\xi\big(N_Y^\xi - 1\big)\big(N_Y^\xi - 2\big) - \bar{k}_5(\tau)N_Y^\xi - \bar{k}_6(\tau)\big) \\
&\quad \times \tilde{P}\big(N_X^\xi, N_Y^\xi\big), \qquad (15)
\end{aligned}$$

where

$$\bar{k}_i(\tau) = k_i(V_c)\frac{1 - e^{-a_0^\xi \tau}}{a_0^\xi}. \quad (16)$$

Multiplying Eq. (15) by N_X^ξ and summing over N_X^ξ and N_Y^ξ yields the discrete time rate equation,

$$\begin{aligned}
\overline{N}_X(t+\tau) - \overline{N}_X(t) &= \big(e^{\tau \frac{\partial}{\partial t}} - 1\big)\overline{N}_X(t) \\
&= \bar{k}_1 - \bar{k}_2\overline{N}_X - \bar{k}_3\overline{N}_X\overline{N}_Y^2 + \bar{k}_4\overline{N}_Y^3, \quad (17)
\end{aligned}$$

where we have introduced the time translation operator $\exp(\tau\frac{\partial}{\partial t})$. Expanding the translation operator in a Taylor series and taking the limit $\tau \to 0$ gives the macroscopic rate law for X in Eq. (11). The chemical concentrations are defined by $c_X = \overline{N}_X/V_c$ and $c_Y = \overline{N}_Y/V_c$ while the rate constants are given by $k_1 = k_1(V_c)/V_c$, $k_2 = k_2(V_c)$, $k_3 = k_3(V_c)V_c^2$, $k_4 = k_4(V_c)V_c^2$, $k_6 = k_6(V_c)/V_c$, $k_5 = k_5(V_c)$. Here we used the fact that $\lim_{\tau\to 0}\bar{k}_i(\tau)/\tau = k_i(V_c)$. Similarly, multiplying by N_Y^ξ and carrying out a similar analysis gives the macroscopic rate law for c_Y.

4. Selkov model simulation results

In order to test the utility of RMPC dynamics, we simulated the dynamics of the Selkov model using the algorithm developed in Section 2. The simulations were carried out for systems whose size ranged from $N_c = 10^3$ to $N_c = 50^3$. From the phase diagram of the Selkov model [29] and our mean field analysis, parameter values corresponding to a stable limit cycle and stable focus could be determined. They are: $k_1 = 0.0009485$, $k_2 = 0.0001$, $k_3 = 0.0004$, $k_4 = 0.0004$, $k_5 = 0.001$, while $k_6 = 0.0001265$ for the limit cycle and $k_6 = 0.0002024$ for the stable focus.

If reactions occur on time scales that are long compared to the velocity relaxation time, as is the case for most reactions of interest, the velocity distribution will be Maxwellian. In our simplified Selkov reaction rule reactive events are thermoneutral and do not depend on particle velocities, so no perturbation of the velocity distribution will occur as a result of reaction. The

Author's personal copy

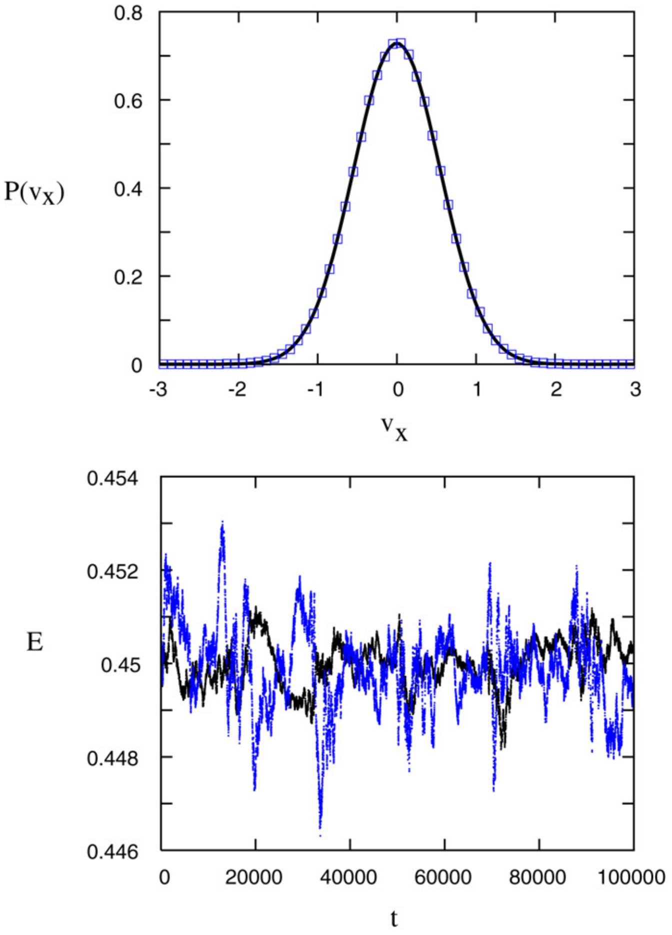

Fig. 1. Velocity distribution and energy for stable limit cycle dynamics. (top) Comparison of the simulated x-component of the velocity distribution of X-particles with a Maxwellian distribution at $k_BT = 0.3$ in a system with $N_c = 50^3$. (bottom) The total energy versus time for $N_c = 30^3$ (blue) and $N_c = 50^3$ (black). (For interpretation of the references to color in this figure legend, the reader is referred to the web version of this article.)

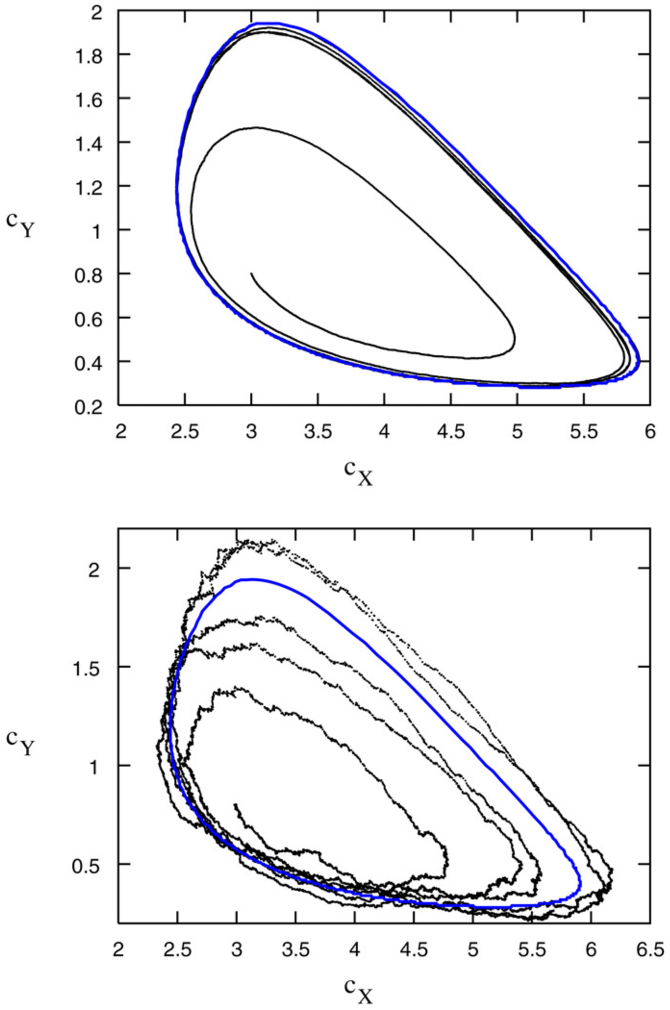

Fig. 2. Phase plane plots of c_X vs c_Y for $0 \leqslant t \leqslant 100000$ showing evolution to a stable limit cycle. (top) $N_c = 50^3$ and (bottom) $N_c = 10^3$. The mean field limit cycle is indicated by a blue line. (For interpretation of the references to color in this figure legend, the reader is referred to the web version of this article.)

Selkov model is an example of a reaction carried out under far-from-equilibrium conditions where the concentrations of some species are assumed to be held fixed by external flows. As a result, particle numbers are not conserved in the dynamics. Consequently, neither the momentum nor energy are conserved, in contrast to non-reactive MPC dynamics. Neither the restriction to reactions that are independent of velocities nor the breakdown of conservation laws need be assumed and the collision rules discussed in Appendix A provide examples where these conditions are not violated. The extent to which the velocity distribution remains Maxwellian and the energy is conserved in this far-from-equilibrium system can be seen in Fig. 1 where the velocity distribution and energy are shown for limit cycle dynamics. The velocity distribution is Maxwellian while the total energy fluctuates about a fixed value. The energy fluctuations are larger for smaller system sizes as expected.

Evolution to stable limit cycle dynamics is shown in Fig. 2 for large ($N_c = 50^3$) and small ($N_c = 10^3$) system sizes. The c_X versus c_Y phase plane plot for $N_c = 50^3$ shows that a stable limit cycle, which closely matches the mean field result, is obtained from RMPC dynamics. Since reaction is much slower than diffusion in our simulation conditions, the system is nearly spatially homogeneous. The degree to which diffusion is able to maintain spatial homogeneity can be gauged by the diffusion length $\ell_D = (D\tau_c)^{1/2}$, where τ_c is a characteristic time scale in the system. Taking τ_c to the period of the limit cycle, $\tau_c \approx 18750$, and using the value of the diffusion coefficient computed from Eq. (2), we find $\ell_D \approx 88$, which is larger than the linear dimension of the system. In addition, the large number of particles in the system leads to small fluctuations so that mean field behavior is expected. For small $N_c = 10^3$ system sizes, fluctuations are much more pronounced and these large fluctuations signal the observed breakdown of the mean field approximation.

Similar trends are seen for parameter values corresponding to a stable focus shown in Fig. 3. For large system sizes oscillatory decay to the focus is observed. For the small system size there are large fluctuations which signal the breakdown of mean field behavior for small systems.

Author's personal copy

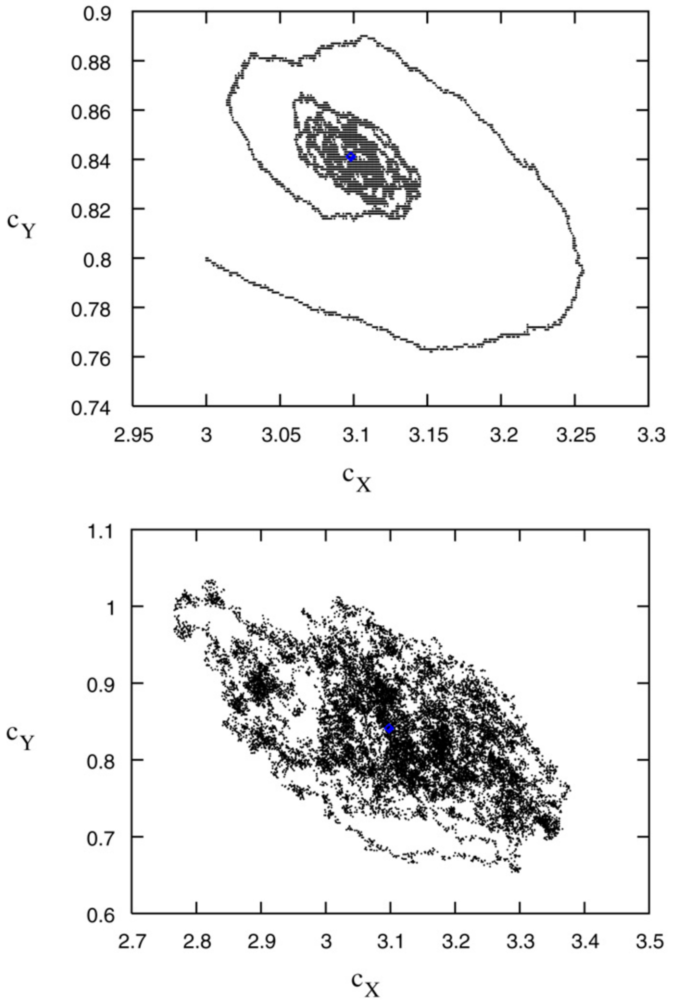

Fig. 3. (top) Oscillatory decay to a stable focus shown as a phase plane plot of c_X vs c_Y for $0 \leqslant t \leqslant 100000$ for $N_c = 50^3$. (bottom) Phase plane plot for $N_c = 10^3$ showing very noisy oscillatory behavior. The mean field fixed point is indicated by a solid blue circle. (For interpretation of the references to color in this figure legend, the reader is referred to the web version of this article.)

5. Conclusion

Reactive multiparticle collision dynamics can be used to study spatially distributed reacting systems in both equilibrium and nonequilibrium conditions. In the simplest version of the model, the reactive events include the creation and destruction of particles. This leads to a violation of the basic conservation laws, in contrast to non-reactive MPC dynamics. Furthermore, the reactive collision model chosen to illustrate the results is especially simple since reaction occurs independently of the particle velocities. In this case, assuming diffusion is rapid compared to reaction, the model is equivalent to a birth–death Markov process dynamics for the species numbers. In this regime the dynamics could have been simulated effectively using the Gillespie algorithm for the birth–death master equation since spatial degrees of freedom play a minor role. However, RMPC need not be restricted to this simple case. Appendix A indicates how the reaction rules can be modified to satisfy mass, momentum and energy conservation. In this case the solvent in which the reactions occur is explicitly taken into account. Such rules can also be adapted to incorporate activated reactive processes.

RMPC dynamics may be contrasted with birth–death master equation dynamics that takes into account spatial degrees of freedom. In such master equation approaches, the system is divided into cells in which stochastic birth–death reactions occur and particles hop from cell to cell by diffusive jumps. RMPC dynamics is similar in spirit except that MPC non-reactive collision dynamics is used to move particles in the system. On long distance and time scales, this dynamics will generate diffusive motion of the species with known values of the diffusion coefficients. Since MPC dynamics is easy and efficient to simulate, it is a very effective way to model these diffusion processes. The algorithm is synchronous, with the time τ governing the non-reactive MPC collisions.

In contrast to spatial master equation approaches, RMPC dynamics provides a more microscopic perspective of the system that can be very useful in many contexts. For example, hybrid MPC-MD schemes have proven to be a very effective way to simulate conformational changes in polymers and biomolecules and colloidal dynamics in solution by combining full molecular dynamics of some relevant species with MPC dynamics of the solvent. The reactive extension presented here can be used in similar contexts where reactions can occur among the solvent molecules, which interact with large solute molecules or for reactions occurring directly with solute molecules. Effects of cellular crowding, where obstacles in the cell influence both transport and reaction, can be studied in this way [30,31]. As a result, the method should prove useful in a variety of applications where molecular motions, reactions and spatial degrees of freedom play a role.

Acknowledgement

This work was supported in part by a grant from the Natural Sciences and Engineering Research Council of Canada.

Appendix A. Reaction rules

In this appendix we give rules for chemical reactive events that conserve mass, momentum, and energy within a similarly constrained background medium. These rules produce dynamical correlations through the imposed conservation constraints. Reactive collisions obey the constraints imposed by fission and fusion of particle pairs and such events are confined to a cell but are not local within a cell. Such birth–death processes can be implemented because coordinates do not appear in the dynamical constraints and potential energy is absent. Below we show in a few examples of typical elementary reactions how reactive collision rules can be constructed. The methods discussed here can be extended to treat other reactions encountered in applications.

Example 1. $A + B \to C$. For structureless A, B and C particles, it is not possible to conserve energy and momentum without an additional particle or particles participating in the reaction. The

Author's personal copy

simplest case to consider is $A + B + M \to C + M$, where M is a solvent particle. For mass conservation we must have $m_C = m_A + m_B$. For energy conservation, the center of mass momentum of an A and B particle is $\mathbf{P}_{AB} = \mathbf{p}_A + \mathbf{p}_B$. Similarly, the relative momentum of the pair is $\mathbf{p}_{AB} = (m_A\mathbf{p}_B - m_B\mathbf{p}_A)/m_C$. Letting primes denote post-collision quantities, energy conservation reads,

$$\begin{aligned} \frac{p_A^2}{2m_A} + \frac{p_B^2}{2m_B} + \frac{p_M^2}{2m_M} &= \frac{P_{AB}^2}{2m_C} + \frac{p_{AB}^2}{2\mu} + \frac{p_M^2}{2m_M} \\ &= \frac{p_C'^2}{2m_C} + \frac{p_M'^2}{2m_M}, \end{aligned} \tag{A.1}$$

where $\mu = m_A m_B/m_C$ is the reduced mass. If $P_{AB}^2/2m_C = p_C'^2/2m_C$ in this equation, then $p_{AB}^2/2\mu + p_M^2/2m_M = p_M'^2/2m_M$. Thus, the original AB pair forms a C particle with the same center of mass energy. Then to conserve total energy the internal energy in the AB pair is transferred to the M particle. These equations determine the magnitudes p'_C and p'_M. For momentum conservation, $\mathbf{p}_A + \mathbf{p}_B + \mathbf{p}_M = \mathbf{p}'_C + \mathbf{p}'_M$. Momentum is conserved even if $\mathbf{p}'_M$ has a randomly chosen direction $\hat{\mathbf{n}}$ provided $\mathbf{p}'_M = \hat{\mathbf{n}}p'_M = \hat{\mathbf{n}}(p_M^2 + m_M p_{AB}^2/\mu)^{1/2}$. The value of $\mathbf{p}'_C$ follows from the equation: $\mathbf{p}'_C = \mathbf{p}_A + \mathbf{p}_B + \mathbf{p}_M - \mathbf{p}'_M$, where (random) $\hat{\mathbf{n}}$ couples $\mathbf{p}'_C$ and $\mathbf{p}'_M$.

Since the initial positions of A, B and M particles are irrelevant, we can either remove both A and B and create a C particle at a random position or we can destroy either A or B and assign the position of the remaining particle to C. The momenta, $\mathbf{p}'_C$ and $\mathbf{p}'_M$, are chosen according to the above prescription.

Example 2. $C + M \to A + B + M$. This reaction is formally the reverse of Example 1 but, if we choose, the conservation laws can be satisfied using different dynamical rules. For mass conservation we again have $m_C = m_A + m_B$. For energy conservation

$$\begin{aligned} \frac{p_C^2}{2m_C} + \frac{p_M^2}{2m_M} &= \frac{p_A'^2}{2m_A} + \frac{p_B'^2}{2m_B} + \frac{p_M'^2}{2m_M} \\ &= \frac{P_{AB}'^2}{2m_C} + \frac{p_{AB}'^2}{2\mu} + \frac{p_M'^2}{2m_M}. \end{aligned} \tag{A.2}$$

Again, let $P_{AB}'^2/2m_C = p_C^2/2m_C$, thereby conserving the energy of the center of mass motion. This implies $p_M'^2/2m_M = p_M^2/2m_M - p_{AB}'^2/2\mu$. However there is freedom of choice in the relative kinetic energy of the AB pair, implying the choice of a specific rule. For momentum conservation, $\mathbf{p}_C + \mathbf{p}_M = \mathbf{p}'_A + \mathbf{p}'_B + \mathbf{p}'_M$. The magnitude p'_{AB}, where $\mathbf{p}'_{AB} = (m_B\mathbf{p}'_A - m_A\mathbf{p}'_B)/m_C$, is determined by our rule and the magnitude p'_M follows from the energy conservation relation. In general we can choose the direction $\hat{\mathbf{n}}$ of $\mathbf{p}'_M$ and $\hat{\mathbf{n}}_{AB}$ of $\mathbf{p}'_{AB}$ randomly, so that $\mathbf{p}'_M = \hat{\mathbf{n}}p'_M$ and $\mathbf{p}'_{AB} = \hat{\mathbf{n}}_{AB}p'_{AB}$. This information allows us to determine $\mathbf{p}'_A$ and $\mathbf{p}'_B$. The simplest rule is to set $\frac{p_{AB}'^2}{2\mu} = 0$, i.e., $p'_{AB} = 0$. Then there is no need for the M particle and we can just consider $C \to A + B$ and still satisfy the conservation laws. In this case we have, from the relative momentum, $\mathbf{p}'_A = m_A\mathbf{p}'_B/m_B$, which then gives $\mathbf{p}'_B = m_B\mathbf{p}_C/m_C$. Example 2 in its full form is the reverse of Example 1. Microscopic detailed balance may be imposed.

Example 3. $A + B \to C + D$. This example can be treated in a similar way to Example 2. For mass conservation, $m_A + m_B = m_C + m_D$. Let $M_{AB} = m_A + m_B$ and $\mu_{AB} = m_A m_B/(m_A + m_B)$, etc. Mass conservation implies $M_{AB} = M_{CD} \equiv M$. For energy conservation

$$\begin{aligned} \frac{p_A^2}{2m_A} + \frac{p_B^2}{2m_B} = \frac{p_C'^2}{2m_C} + \frac{p_D'^2}{2m_D} &= \frac{P_{AB}^2}{2M} + \frac{p_{AB}^2}{2\mu_{AB}} \\ &= \frac{P_{CD}'^2}{2M} + \frac{p_{CD}'^2}{2\mu_{CD}}. \end{aligned} \tag{A.3}$$

For momentum conservation, $\mathbf{p}_A + \mathbf{p}_B = \mathbf{p}'_C + \mathbf{p}'_D$, or $\mathbf{P}_{AB} = \mathbf{P}'_{CD}$. Momentum conservation implies that $P_{AB}^2/2M = P_{CD}^2/2M$. Energy conservation gives $p_{AB}^2/2\mu_{AB} = p_{CD}'^2/2\mu_{CD}$. This equation determines the magnitude of the relative kinetic energy of the CD pair: $p'_{CD} = (\mu_{CD}p_{AB}^2/\mu_{AB})^{1/2}$. Choose the direction of $\mathbf{p}'_{CD}$ at random. Call this direction $\hat{\mathbf{n}}_{CD}$. Thus, $\mathbf{p}'_{CD} = \hat{\mathbf{n}}_{CD}(\mu_{CD}p_{AB}^2/\mu_{AB})^{1/2}$. Note that $\mathbf{p}'_{CD} = \mu_{CD}(\mathbf{p}'_C/m_C - \mathbf{p}'_D/m_D) = \mathbf{p}'_C - \mu_{CD}/m_D \cdot \mathbf{P}'_{CD}$. Since $\mathbf{P}'_{CD}$ and $\mathbf{p}'_{CD}$ are known $\mathbf{p}'_C = \mathbf{p}'_{CD} + \mu_{CD}/m_D \cdot \mathbf{P}'_{CD}$. The value of $\mathbf{p}'_D$ follows from momentum conservation.

Comparison of the reaction rules defined in this appendix with those used in the Selkov-model simulations illustrates that chemical reactions within a mesoscopic hydrodynamic evolution can be simulated with different degrees of realism. In the Selkov simulation the creation and destruction of particles is not hydrodynamically conservative. In general, chemical reactions with sources can be simulated by changing solvent particles into reagents or reactive particles into inert species; this conserves dynamical variables. Also, this preserves particle number locally but not particle identity. In open systems, faithful simulation of source and sink chemical processes requires additional considerations. Introduction of reagents and removal of products can occur either at the boundaries of a homogeneous system or in the bulk for a heterogeneous system. Evidently, an open reaction can be simulated by careful imitation of the appropriate boundary conditions. The developments described in this appendix indicate how chemical and dynamical realism can be improved even to the extent of accounting for reaction energy and local temperature changes.

References

[1] C.V. Rao, D.M. Wolf, A.P. Arkin, Control, exploitation and tolerance of intracellular noise, Nature 420 (2002) 231–237.

[2] G. Nicolis, I. Prigogine, Self-Organization in Nonequilibrium Systems, Wiley, New York, 1977.

[3] D.T. Gillespie, Exact stochastic simulation of coupled chemical reactions, J. Phys. Chem. 81 (1977) 2340–2361.

[4] D.T. Gillespie, Approximate accelerated stochastic simulation of reacting systems, J. Chem. Phys. 115 (2001) 1716–1733.

[5] A.B. Stundzia, C.J. Lumsden, Stochastic simulation of coupled reaction–diffusion processes, J. Comput. Phys. 127 (1996) 196–207.

[6] T.S. Shimizu, N. Le Novère, M.D. Levin, A.J. Beavil, B.J. Sutton, D. Bray, Molecular model of a lattice of signalling proteins involved in bacterial chemotaxis, Nat. Cell Biol. 2 (2000) 792–796.

Author's personal copy

[7] J. Elf, A. Doncic, M. Ehrenberg, Mesoscopic reaction–diffusion in intracellular signaling, Proc. SPIE 5110 (2003) 114–124.
[8] S.S. Andrews, D. Bray, Stochastic simulation of chemical reactions with spatial resolution and single molecule detail, Phys. Biol. 1 (2004) 137–151.
[9] J.S. van Zon, P.R. ten Wolde, Green's-function reaction dynamics: a particle-based approach for simulating biochemical networks in time and space, J. Chem. Phys. 123 (2005) 234910.
[10] J.V. Rodriguez, J.A. Kaandorp, M. Dobrzynski, J.G. Blom, Spatial stochastic modelling of the phosphoenolpyruvate-dependent phosphotransferase (PTS) pathway in Escherichia coli, Bioinformatics 22 (2006) 1895–1901.
[11] A. Malevanets, R. Kapral, Mesoscopic model for solvent dynamics, J. Chem. Phys. 110 (1999) 8605–8613.
[12] A. Malevanets, R. Kapral, Solute molecular dynamics in a mesoscale solvent, J. Chem. Phys. 112 (2000) 7260–7269.
[13] R. Kapral, Multiparticle collision dynamics: simulation of complex systems on mesoscales, Adv. Chem. Phys. (2008), in press.
[14] K. Tucci, R. Kapral, Mesoscopic model for diffusion-influenced reaction dynamics, J. Chem. Phys. 120 (2004) 8262–8270.
[15] T. Ihle, E. Tüzel, D.M. Kroll, Equilibrium calculation of transport coefficients for a fluid-particle model, Phys. Rev. E 72 (2005) 046707.
[16] C.M. Pooley, J.M. Yeomans, Kinetic theory derivation of the transport coefficients of stochastic rotation dynamics, J. Phys. Chem. B 109 (2005) 6505–6513.
[17] E. Allahyarov, G. Gompper, Mesoscopic solvent simulations: multiparticle-collision dynamics of three-dimensional flows, Phys. Rev. E 66 (2002) 036702(9).
[18] J.T. Padding, A.A. Louis, Hydrodynamic interactions and Brownian forces in colloidal suspensions: coarse-graining over time and length scales, Phys. Rev. E 74 (2006) 031402(29).
[19] K. Mussawisade, M. Ripoll, R.G. Winkler, G. Gompper, Dynamics of polymers in a particle-based mesoscopic solvent, J. Chem. Phys. 123 (2005) 144905(11).
[20] N. Kikuchi, J.F. Ryder, C.M. Pooley, J.M. Yeomans, Kinetics of the polymer collapse transition: the role of hydrodynamics, Phys. Rev. E 71 (2005) 061804(8).
[21] D.J. Earl, C.M. Pooley, J.F. Ryder, I. Bredberg, J.M. Yeomans, Modeling microscopic swimmers at low Reynolds number, J. Chem. Phys. (2007) 064703(10).
[22] G. Rückner, R. Kapral, Chemically powered nanodimers, Phys. Rev. Lett. 98 (2007) 150603(4).
[23] K. Rohlf, Stochastic phase-space description for reactions that change particle numbers, J. Math. Chem. (2008), in press.
[24] K. Tucci, R. Kapral, Mesoscopic multiparticle collision dynamics of reaction–diffusion fronts, J. Phys. Chem. B 109 (2005) 21300–21304.
[25] E.E. Selkov, Self-oscillations in glycolysis 1. A simple kinetic model, Eur. J. Biochem. 4 (1968) 79–86.
[26] R. Kapral, A. Lawniczak, P. Masiar, Reactive dynamics in a multispecies lattice-gas automaton, J. Chem. Phys. 96 (1992) 2762–2776.
[27] J.P. Boon, D. Dab, R. Kapral, A. Lawniczak, Lattice gas automata for reactive systems, Phys. Repts. 273 (1996) 55–147.
[28] B. Hasslacher, R. Kapral, A. Lawniczak, Molecular Turing structures in the biochemistry of the cell, Chaos 3 (1993) 7–13.
[29] P.H. Richter, P. Rehmus, J. Ross, Control and dissipation in oscillatory chemical engines, Prog. Theor. Phys. 66 (1981) 385–405.
[30] S. Schnell, T.E. Turner, Reaction kinetics in intracellular environments with macromolecular crowding: simulations and rate laws, Prog. Biophys. Molec. Biol. 85 (2004) 235–260.
[31] C. Echevería, K. Tucci, R. Kapral, Diffusion and reaction in crowded environments, J. Phys.: Condens. Matter 19 (2007) 065146(12).